Notice Warning Concerning Copyright Restrictions

Surface and Coatings Technology, 61 (1993) 108–114

Processes in plasma arc installation for vacuum coating depositions
Part 2. Plasma propagation

Vladimir I. Gorokhovsky
Mirus International Inc., 801 Sheppard Avenue West, North York, Ont., M3H 2T3 (Canada)

Abstract

This paper presents the results of investigation of the propagation of plasma flow in a plasma arc installation for vacuum coating deposition. The distribution of plasma arc flow parameters in longitudinal and curvilinear magnetic fields is analysed. The dependence of the concentration of various atomic particles on the parameters of the vacuum arc plasma was investigated by emission spectroscopy techniques. It was found that in a vacuum arc jet the various elements comprising the cathode, and their isotopes, separate in the presence of a magnetic field. The concentration of atomic particles—the products of molecular dissociation—depends on the arc-penetrating current through the working chamber area. The plasma sheath created near the substrates under negative bias potential was investigated. The criteria for the placement of filters to capture droplets and their probabilistic efficiency were determined for various filter geometries. The results of the application of this process to coating deposition technology are discussed.

1. Introduction

As is known, the utilization of vacuum arcs (VAs) or arcs of low pressure intensifies significantly the process of vacuum deposition of coatings. In the technological volume of plasma arc installations (PAIs), besides the metallic plasma generation, complex physical–chemical processes connected with the action of external electromagnetic fields and other factors take place. The second part of the present work is devoted to a consideration of these processes.

2. Experimental details

The key results presented below were obtained at the Thermion-500 installation (PAI-2) and the PAI-3 installation with a copper cold cathode (CC). The description of the installation and some of the measurement methods are given in Part 1 of this study. The concentrations of the plasma components were determined by the optical actinometry method [1, 2]. For this purpose, a special gas actinometer is introduced into the plasma. Comparing the radiation intensity of the spectral line I_i of the plasma component with the line intensity I_a of the gas actinometer, it is possible to obtain the desired concentration N_i:

$$N_i = \eta(I_i/I_a)N_a \tag{1}$$

where η is a constant and N_a is the concentration of the gas actinometer.

The characteristics of coatings were studied by standard methods, *i.e.* the morphology of coatings was investigated with the help of a Neophot-2 optical microscope and a scanning electron microscope [3]. The phase composition of carbon coatings was studied by photoelectron and Raman spectroscopy.

3. Results and discussion

3.1. Arc in a longitudinal magnetic field

An investigation of the arc behaviour in a magnetic field was performed at the PAI-3 installation with a copper CC. A description of the installation and some of the results obtained are presented in refs. 4 and 5. In supersonic plasma jets generated by VA, mean values of conductivity and electron temperature T_e have been measured. It follows from the data in Fig. 1(a) that the magnetic field significantly influences these parameters. The relationship between the measured values of σ and T_e may be described by Spitzer's formula [6] ($\sigma \propto T_e^{3/2}$) which confirms a high degree of ionization in the VA plasma. Figure 1(b) demonstrates that the current transfer in the VA column is, in general, determined by the field mode. For the connection between E_z and j_z we can write $j_z = \sigma E_z$. In the case of a simple channel model with $\sigma =$ constant, we have $E_z = \sigma I_a/S_\sigma$, where I_a is the arc current and S_σ is the conductivity zone area.

In order to obtain the structure of the plasma column, measurements were performed of mass flow, ion current density and radiation spectra of different components as well as other parameters. It was established that the presence of a magnetic field leads to a plasma flow

0257-8972/93/$6.00

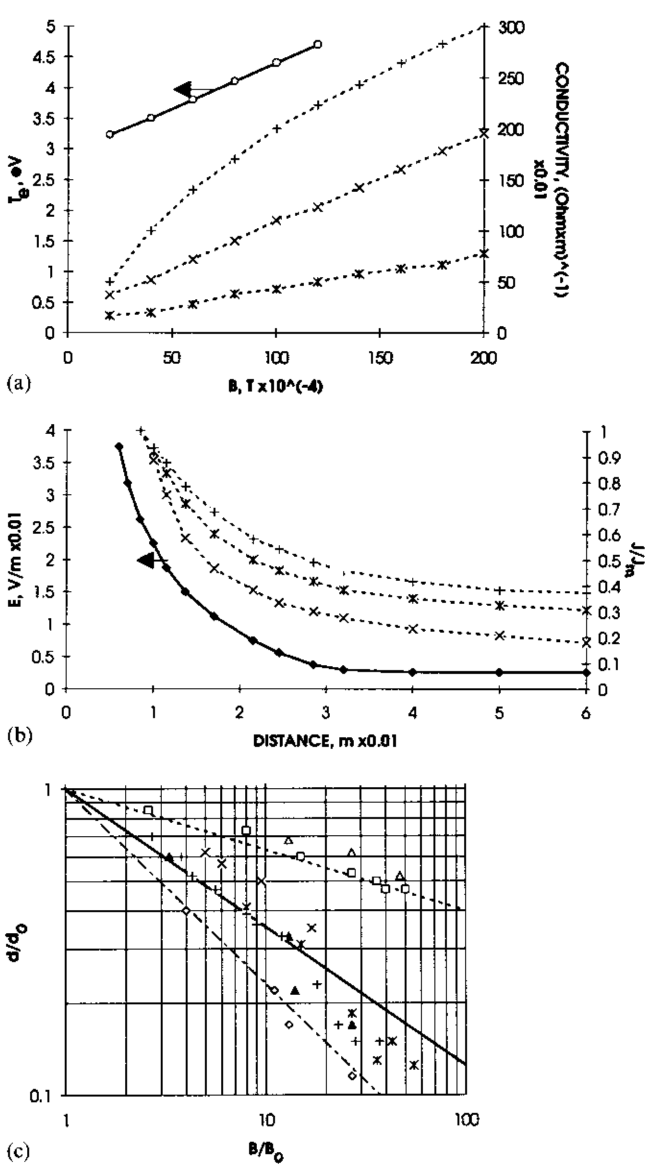

Fig. 1. Parameters of the VA in a longitudinal magnetic field: (a) dependences of electrical conductivity σ and electron temperature T_e (○) for the VA with copper CC on the magnetic field intensity B (σ is shown for distances L from the cathode) of 0.015 m (*), 0.045 m (x) and 0.115 m (+)); (b) electric field E (◆), and the ratio of the arc current density J along the arc column axis to the current density (J_m at a distance of 1 cm from the cathode for magnetic fields of 20 G (x), 60 G (*) and 120 G (+); (c) dependence of the relative diameters d/d_0 of different zones of the VA with a copper CC on the magnetic field intensity B/B_0, measured by optical (▲, Cu^+ (248.9 nm); ◇, Cu^{2+} (245.2 nm); △, Cu atoms (249.1 nm); □, visible diameter) and probe (induction sensor with $I_a = 80$ A (*) and 60 A (+), and Langmuir probe (x)) methods (-·-, $d/d_0 = (B/B_0)^{-0.7}$;—, $d/d_0 = (B/B_0)^{-0.5}$; - - -, $d/d_0 = (B/B_0)^{-0.2}$).

concentration that increases with the growth of the magnetic field intensity. Figure 1(c) presents the dependences of diameters of different arc column zones on the intensity of the magnetic field B.

The experimental analysis showed that with the presence of the field one could distinguish a central conductivity zone consisting of highly ionized plasma and a peripheral zone mainly consisting of neutral atoms. In turn, there is the central core where multicharged ions prevail and the external zone is filled essentially by singly charged ions. This spatial ion distribution may be explained if one takes into account the separation of the ions due to the plasma flow rotation in the magnetic field. This rotation may be found simply by observing the pattern of ion deposition on the thin plates placed along the arc axis [6]. At a distance from the VA cathode, a broadening of the plasma flow in the radial direction takes place. This broadening is determined by the plasma diffusion in the magnetic field. The results show that the jet core filled by the laminar plasma widens following approximately the law of classical diffusion with a diffusion coefficient $D_e \propto 1/B^2$. The external boundary of the conductivity zone widens in accordance with the law of turbulent diffusion with the Bohm diffusion coefficient $D_B \propto 1/B$. This indicates the presence of turbulence of the plasma near the arc column boundary [7].

3.2. Plasma separation

The flows of the VA plasma of a CC usually contain macroparticles of the cathode material that may contaminate the properties of coatings. To separate the plasma from macroparticles, electromagnetic macroparticle filters (EMFs) provide a transportation path by turning the plasma along the curved magnetic field lines of force. The macroparticles moving along the rectilinear trajectories are deposited at the filter walls.

Monte Carlo computer modelling methods were used to define the probability of trajectories of macroparticles through the EMF. Figure 2(a) presents the schematic of an angular-shaped EMF and particle trajectories after four collisions with EMF walls. Figure 2(b) presents a photograph of the plasma arc column (with CC-type source) in the quarter-torus magnetic field of the angular-shaped EMF. The plasma movement in the EMF has a complicated character. To describe this movement the single-particle plasma–optical approximation has been used in refs. 8–10. The containment of plasma ions in the EMF was explained by the appearance of an electric field between the positively charged filter wall and a cloud of magnetized electrons. The plasma–optical filters are effective for the transportation of ions from the central VA zone at a rather low pressure. The numerical modelling performed in refs. 10 and 11 revealed deviations from the simplified plasma–optical model displayed in the diffusive character of plasma propagation. If the cross-section of the VA is less than the characteristic EMF dimension it is possible to design a diffusive-type filter. To define the character of plasma movement in this case at the Thermion installation an investigation

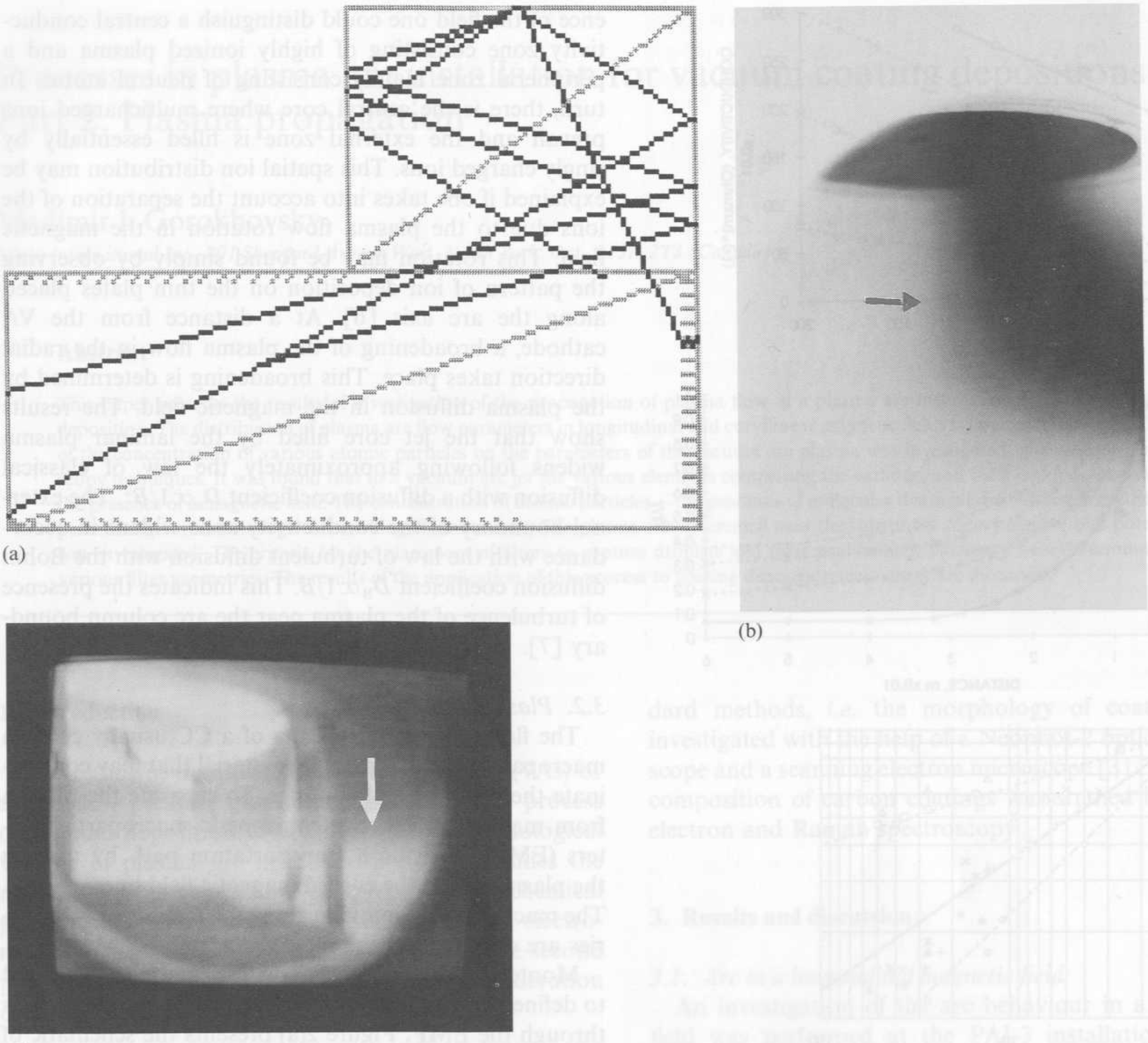

Fig. 2. Modelling of VA with a CC in an angular EMF: (a) computer simulation of macroparticle trajectories in an angular E.M.F. in the x–y projection (grey lines are the boards of the macroparticle filter surfaces; black lines are the trajectories of macroparticles, which had started with a random angular distribution); (b) photograph of the VA column in an angular EMF (the arrow shows the position of the VA column); (c) photograph of the VA with graphite HEC in the EMF with opposing magnetic field of the Thermion installation (the arrow shows the position of the VA column).

was performed of VA at a hot evaporating cathode (HEC) from graphite in the opposing magnetic fields of the EMF. Figure 2(c) presents the photograph of such an arc. This representation has a structure which is characteristic for an arc in a longitudinal magnetic field. It is also similar to the case shown in Fig. 2(b). The arc axis is disposed along the magnetic field line that intersects the cathode surface in the zone of the cathode fixing (similar to the case shown in Fig. 1(b), Part 1 (*Surf. Coat. Technol.*, *61* (1993) 101)). The movement of plasma ions in the diffusive filter may be expressed as follows: in the longitudinal direction it is a movement with a supersonic velocity gained in the near-cathode VA region; in the lateral direction it is diffusion with a diffusion coefficient $D_B \propto 1/B$. It is interesting to note that in the arc column of the VA with a HEC high energy ions are absent. However, propagation of this arc plasma in a curvilinear magnetic field is similar for plasma arc jet flow from the cathodic spots of VA with a CC.

The investigation revealed a number of peculiarities of this movement. First, the arc column shifts in a transverse direction which may be explained by the centrifugal drift of magnetized electrons in the $E \times B$ fields [7]. Second, a special division of ions with different specific charges q/M takes place. The effect of the division was investigated in PAI-2 (Fig. 1(a), Part 1) for VA fired at a CC from an Fe–Ni alloy with a ratio of concentrations $k(\mathrm{Ni{-}Fe}) = C_{\mathrm{Ni}}/C_{\mathrm{Fe}} = 0.56$. The plasma flow of this VA was passed through an angular filter. The ratio k(Fe–Ni) in the plasma was determined by the measured ratio of intensities of atomic lines of these elements (by the optical actinometry method). Furthermore, the composition of films deposited from the plasmas was measured. The experiments demonstrated that the composition of films obtained at the entrance to the plasma in an EMF corresponds to the cathode composition.

At the same time, films were obtained at the exit of the filter with a composition of $k(\mathrm{Fe{-}Ni}) = 0.25$. Simultaneously, the plasma flow itself had a composition of $k(\mathrm{Fe{-}Ni}) = 0.19$ at the exit of the filter measured by the optical actinometry method. Also, the process in an EMF using opposing magnetic fields produced by two solenoids (in PAI-3) (Fig. 1(b), Part 1) was investigated. In this EMF the plasma flow produced by VA on a CC formed from Co–Ni alloy was directed. The pressure of the Ar–N_2 mixture in the working chamber was varied from 5×10^{-3} up to 8×10^{-1} Pa. The plasma composition was defined by a mass spectrometer. From the data obtained, it is evident that an increase of magnetic field intensity on the fixed magnetic flux lines leads to an increase in the concentration of both metal and gas ions (Fig. 3(a)). This effect may be explained by a compression of the VA column in the magnetic field and is similar to VA in the longitudinal magnetic field. As can be seen from the data in Fig. 3(a), the ratio of Ni isotope concentrations at the filter exit $k(^{60}\mathrm{Ni}^+{-}^{58}\mathrm{Ni}^+)$ with fixed magnetic flux lines of an oppositely shaped EMF does not depend on B. However, when there is a change of this configuration, the value of $k(^{60}\mathrm{Ni}^+{-}^{58}\mathrm{Ni}^+)$ varies from 1.69 up to 2.16. These values significantly differ from the value $k(^{60}\mathrm{Ni}^+{-}^{58}\mathrm{Ni}^+) = 2.59$ measured in the cathode. Let us note that the value of k for isotopes of Ni in films deposited from the plasma at the EMF entrance corresponds to the values for the cathode material. Simultaneously, for films at the filter exit $k(^{60}\mathrm{Ni}^+{-}^{58}\mathrm{Ni}^+) = 1.8$. Thus, for the filter considered, the obvious effect of a division of the cathode material components is observed.

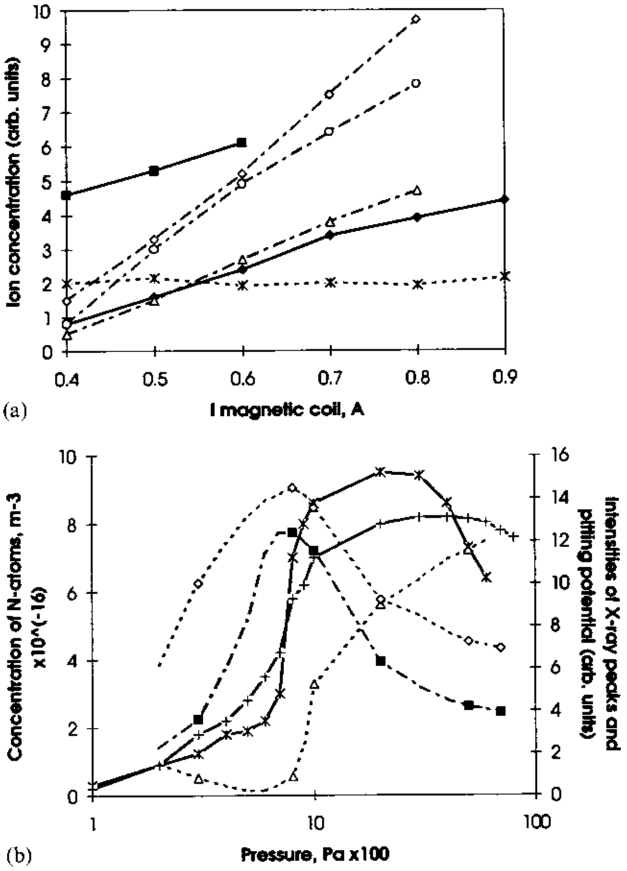

Fig. 3. Concentration of ions in the VA plasma and properties of coatings: (a) the ion concentration is measured in the area near a selected magnetic force line of the opposing magnetic field (■, Ar^+; ◆, N_2^+; ◇, $^{59}Co^{2+}$; ○, $^{58}Ni^{2+}$; △, $^{60}Ni^{2+}$; *, $[[N^+]/([N^+ + N_2{}^+])] \times 10$); (b) concentration of N atoms in a plasma arc flow at the exit of the angular EMF (*, experimental; +, theoretical), intensities of characteristic X-ray peaks from the TiN coating on the Cu substrates (◇, I (Cu); △, I (N)) and the pitting potential for the TiN coating deposition process (–––), using a cold cathodic VA source with angular EMF.

3.3. Plasma arc activation of gases

The experiments demonstrated that VA excites reacting gases introduced into the vacuum volume. In particular, the dissociation of molecular components is very effective. Figure 3(b) represents the concentration of nitrogen atoms C_N produced due to the N_2 dissociation at the angular EMF exit (in PAI-2) (Fig. 1(a), Part 1), as a function of the general pressure P for the arc at a CC made from titanium. This concentration was measured by the optical actinometry method for atomic N lines NI 410 and 411 nm and with argon as gas actinometer ($\lambda = 415.9$ nm). With rising P this concentration sharply increases and reaches a maximum at $P \approx 10^{-1}$ Pa. Experience suggests that this dependence may be explained if the creation of primary channels for N atoms is a dissociative recombination of N_2^+ ions and direct dissociation of N_2 by electron impact with the decay channel—heterogeneous recombination of atoms. Thus C_N may be found from the following expression:

$$C_N = (C^+_{N_2} N_e K^{ei} + C_{N_2} N_e k^d)/(\varepsilon D_N/L) \quad (2)$$

where $C^+_{N_2}$, C_{N_2} and N_e are the concentrations of N_2^+, N_2 and electrons; $\varepsilon \approx 1$ is the coefficient of heterogeneous recombination of N atoms on steel; k^{ei} and k^d are the constants of the reactions of dissociative recombination of N_2^+ ions and direct dissociation of N_2 molecules by electron impacts; D_N is the diffusion coefficient and L

the diffusive length [1,2]. As follows from the data in Fig. 3(b) the TiN coating deposition rate by filtered arc plasma and the concentration of Ti^+ ions at the EMF exit decrease with increases in the general pressure P. The variation in the rate of TiN coating deposition and the protective properties of such coatings correlate with a dependence of the concentration N upon pressure P.

The activation processes are significantly intensified if the auxiliary arc discharge is fired in the working chamber of the installation. This discharge used a plasma of the VA locked in an angular-shaped EMF with a switched-off magnetic system, like a virtual cathode, and an additional anode in the working chamber near the substrates. Figure 4(a) illustrates the influence of the additional arc discharge current on the ion current measured after the exit flange of the angular EMF and shows nitrogen ionization in the additional discharge. The results obtained show that the additional discharge rather homogeneously fills the installation working volume. The electron temperature and the electrical conductivity of such a plasma take on values which are characteristic of highly ionized states, but current transfer determines both the field and the diffusive mode.

The investigations performed showed that in the plasma activated by the additional discharge it is possible to make an effective chemical–thermal treatment of material. An example is the nitriding of high speed steels. According to the data of Fig. 4(a) the nitriding layer depth increases with the growth of nitrogen activation. The microhardness of the steel after nitriding reached 13 GPa from an initial microhardness of 7.5 GPa.

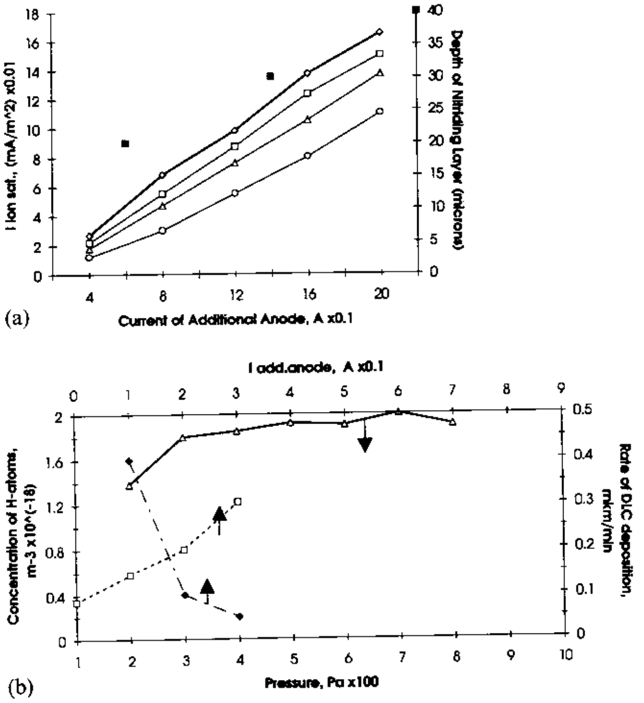

Fig. 4. Influence of auxiliary arc discharge on the parameters of the VA coating deposition process: (a) influence of the current of the additional arc discharge on the ion current in the plasma (◇, 3×10^{-4} h Pa; □, 5×10^{-4} h Pa; △, 7×10^{-4} h Pa; ○, 2×10^{-3} h Pa) and on the depth of the nitriding layer on the high speed steel substrates (■); (b) dependences of the concentration of H atoms on the current from the additional anode $C_H(I)$ (□) and on the hydrogen pressure $C_H(P)$ (△), and of the rate of DLC deposition (◆) in the carbon VA with HEC in the opposing magnetic field of the Thermion installation.

Also, the effect of activation is important for the deposition of coatings. This effect was studied in a deposition of diamond-like coatings (DLCs) at the Thermion installation with an HEC of graphite. The current of the VA with an HEC of graphite was $I_a = 20$ A. The separation of a carbon arc plasma from multi-atom clusters in the EMF with an opposing magnetic field was applied (see Fig. 1(a)). In these experiments the activation of the reacting gas (H_2) was used in the additional discharge with an r.f. bias potential (about -500 V, $f = 1.76$ MHz) applied to the metallic substrate. Figure 4(b) demonstrates the dependence of the concentration of hydrogen atoms C_H and the rate of DLC deposition on the parameters of the additional discharge. The concentration of H atoms was measured by the optical actinometry method for the H line HI 434 nm with an Ar-like gas actinometer ($\lambda = 430$ nm, $P_{Ar} \leqslant 0.05$Pa). C_H may be theoretically described similarly to C_N (see eqn. (2)). A growth of the discharge current leads to an increase of C_H. With the current of the additional discharge greater than 40 A, instead of a deposition an intensive etching of the surface takes place. Thus by changing the concentration C_H it is possible to control the relationship between the rates of etching and deposition. This is critical for the deposition of DLCs [12].

According to investigations performed by the Raman scattering method the DLCs obtained may be described as amorphous films with the sp^3–sp^2 mixed system of fragmentary situated bonds. The ratio of concentrations of sp^3 and sp^2 bonds varied from some units by up to 20%–30% and is dependent on the bias potential and concentration of C_H. The microhardness of coatings deposited on the tungsten carbide inserts (type MS 321) varied in the range 15–30 GPa. Additionally, films with a high concentration of sp^3 bonds resulted in a high microhardness. As a consequence of these initial test results, we may anticipate promising results from the Thermion installation for the process of superhard coating deposition, especially for complex compound coatings (such as cubic BN, TiB_2 etc.).

3.4. *Interaction of the plasma with a negatively charged substrate*

During the deposition of coatings a negative bias potential $U < -100$ V is usually applied to the substrates. Many details of the phenomena caused by the interaction of the VA plasma with the substrate have not been clarified until now. At the same time, these phenomena may influence the deposition of coatings.

In this work an investigation of the plasma layers appearing near the surface of substrates or probes was performed. Figure 5(a) shows a photograph of the plasma layers around cylindrical probes at a potential $U = -350$ V placed in the N–T VA plasma at a pressure of about 10^{-2} Pa. The photograph was obtained using an X-ray pinhole camera registering radiation quanta with an energy greater than 200 eV. Figure 5(b) demonstrates that near a substrate surface there is a sharp growth both of electron concentration N_e and of plasma radiation in the visible range of the spectrum [13]. Thus in the narrow layer near the substrate surface the plasma parameters significantly increase. The characteristic thickness of the plasma layer is $l_p \approx 1$ cm. It is essential that the value of l_p is much more than the Debye length $r_D \approx (T_e/N_e)^{1/2}$ but much less than the free electron length l_e. When analysing the processes of the plasma–surface interaction it is demonstrated that near the surface of a negatively charged substrate there must appear a near-cathode layer of the non-sustained glow discharge with a characteristic thickness $d_c \approx l_p$. Electrons emitted from the negatively charged substrate surface due to secondary emission processes when moving in the near-cathode layer of the glow discharge acquire energy determined by the potential U. If a scattering of the electron energy occurs due to impacts, it must be the case that $d_c > l_e$. However, in these experiments we have $l_p \propto d_c << l_e$. To explain this result it may be assumed that scattering of electrons takes place not at impacts but at the plasma Langmuir oscillations. Therefore the relaxation length of energy $l_{1/2}$, according to ref. 14, is

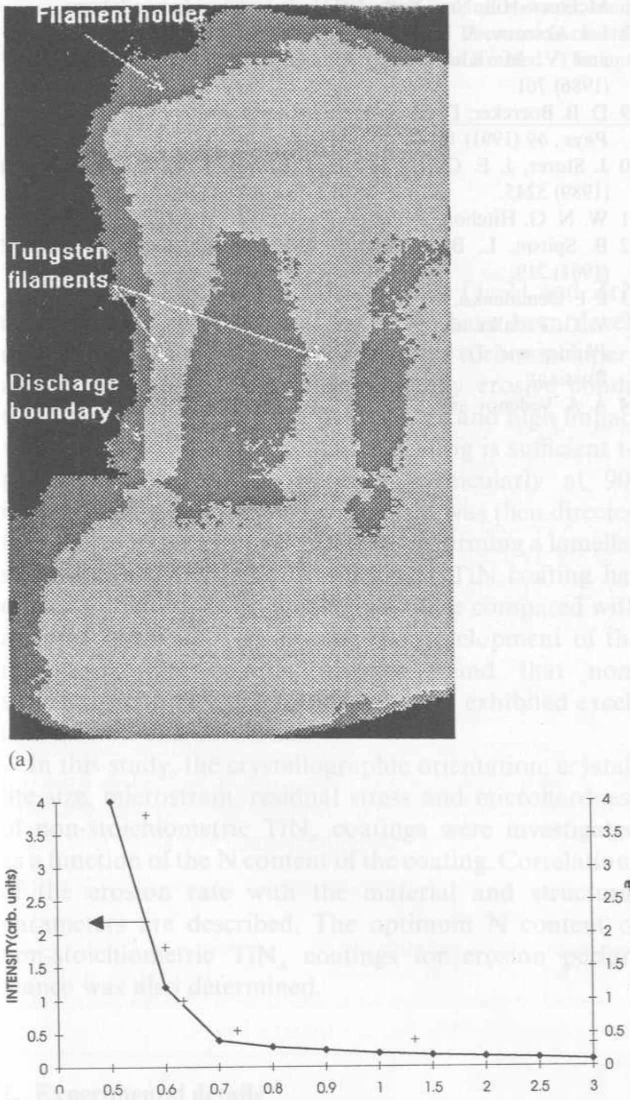

Fig. 5. Plasma layer near a negatively charged substrate in the Ti–N$_2$ VA: (a) X-ray photograph of plasma layers near cylindrical probes at the bias potential $U = -350$ V (computer edited image); (b) distribution of electron concentration (+) and radiation intensity (◆) of Ti^{2+} ions ($\lambda = 256.3$ nm, $P_{N_2} = 6.6 \times 10^{-2}$ Pa) near a negatively charged substrate surface [13].

$$l_{1/2} \approx 0.2(j_{ex}/j_{is})(V_{Te}/\omega_{pe})(\ln \Lambda/\gamma) \qquad (3)$$

where j_{ex} is the density of the random electron current, γ is the coefficient of secondary electron emission, V_{Te} and ω_{pe} are the thermal velocity and electron plasma frequency, and Λ is the Coulomb logarithm.

The evaluation of eqn. (3) leads to $l_{1/2}$ values which qualitatively correspond to the l_p values measured. Thus in the plasma layer near the substrate surface intensive Langmuir oscillations may appear. This must be taken into account when analysing and optimizing processes for vacuum plasma deposition of coatings.

4. Conclusion

Experimental and theoretical investigations of processes taking place within the plasma propagation in the technological volume of PAIs have been performed. The consideration of diffusive approach phenomena in the arc column is suggested. The diffusive model was used to explain the behavior of VA plasma in both longitudinal and curvilinear magnetic fields, when the "flux-tube" model condition could not be utilized. The diffusive model was used to develop high productivity macroparticle filters for VA plasma sources. Also, this model explains the behaviour of diffusive plasma flow from a VA source with an HEC. It is shown that an auxiliary discharge between the arc plasma column and an additional anode provides a significant increase in the activity of reacting gases. Peculiarities of processes in the plasma near the substrate surface are revealed. The results obtained were used for the development and optimization of characteristics of a pilot PAI, the "Thermion-500/SHC", for the deposition of superhard coatings. Based on these results we expect that the Thermion-500/SHC installation will find the most effective application for the processes of complex compounded superhard coating deposition.

Acknowledgments

Most of the results presented in this paper were obtained during the period 1985–1992 in the Institute for Superhard Materials of the Ukrainian Academy of Sciences, Institute for High Temperature of the Russian Academy of Sciences, and in the MS Russia Company. We are indebted to O. Z. Popov for his support of the experimental facilities. Thanks to G. N. Kurtinina and M. S. Pekker for help in the optical measurements and software. The authors are very thankful to V. V. Makarov of MS (Russia) and J. Q. Steigelman of Valenite (USA) for financial support during the concluding part of this work as well as to D. G. Bhat for useful discussions and help in testing of the carbon coatings. The authors would like to thank the principal of Mirus International Inc. for the technical and financial support without which the fulfilment of this work would not be possible.

References

1 V. I. Gorokhovsky and G. N. Kurtinina, *High Energy Chem.*, *23* (1988) 239 (in Russian).

2 V. I. Gorokhovsky and D. K. Otorbaev, *Phys. Chem. Mater. Treat.*, 2 (1989) 51 (in Russian).

3 N. V. Novikov, V. I. Gorokhovsky and B. A. Uryukov, *Surf. Coat. Technol.*, *47* (1991) 770.

4 V. I. Gorokhovsky, V. P. Elovikov, P. L. Lizunov and S. A. Pantyukhin, *Teplophys. Vys. Temp.*, *26* (1988) 239 (in Russian).

5 V. I. Gorokhovsky and V. P. Elovikov, Zh. *Tekh. Phis.*, *57* (1987) 2267 (in Russian).

6 V. I. Gorokhovsky, V. P. Elovikov and B. A. Uryukov, Expansion in vacuum of erosion d.c.-arc plasma, *Proc. XVI Int. Conf. on Phenomena in Ionized Gases, Dusseldorf*, 1983.

7 N. A. Krall and A. W. Trivelpiece, *Principles of Plasma Physics*, McGraw-Hill, New York, 1973.

8 I. I. Aksenov, A. N. Belokhvostikov, V. G. Padalka, N. S. Repalov and V. M. Khoroshikh, *Plasma Phys. Controlled Fusion*, *28* (1986) 761.

9 D. B. Boercker, D. M. Sanders, J. Storer and S. Falabella, *J. Appl. Phys.*, *69* (1991) 115.

10 J. Storer, J. E. Galvin and I. G. Brown, *J. Appl. Phys.*, *66* (11) (1989) 5245.

11 W. N. G. Hitchon, *J. Plasma Phys.*, *38* (1) (1987) 87.

12 B. Spitsin, L. Boilov and B. Derjaguin, *J. Cryst. Growth*, *52* (1981) 219.

13 I. I. Demidenko, N. P. Dikiy, V. D. Ovcharenko, N. S. Lomino, V. G. Padalka and G. N. Polyakova, in *Preprints of the Charkov Physics and Technology Institute*, Vol. 86–27, Charkov, 1986 (in Russian).

14 A. A. Vedenov and D. D. Ryutov, *Rev. Plasma Phys.*, *6* (1980).